
Customized Handling of Unintended Interface Operation in Assistive Robots

Deepak Gopinath*

Northwestern University, Shirley Ryan AbilityLab
Chicago, Illinois
deepakgopinath@u.northwestern.edu

Mahdieh Nejati Javaremi*

Northwestern University, Shirley Ryan AbilityLab
Chicago, Illinois
m.nejati@u.northwestern.edu

Brenna D. Argall

Northwestern University, Shirley Ryan AbilityLab
Chicago, Illinois
brenna.argall@northwestern.edu

ABSTRACT

Teleoperation of physically assistive machines is usually facilitated by interfaces that are low-dimensional and have unique physical mechanisms for their activation. Accidental deviations from intended user input commands due to motor limitations can potentially affect user satisfaction and task performance. In this paper, we present an assistance system that reasons about a human's intended actions during robot teleoperation in order to provide appropriate corrections for unintended behavior. We model the human's physical interaction with a control interface during robot teleoperation using the framework of *dynamic Bayesian Networks* in which we distinguish between *intended* and *measured* physical actions explicitly. By reasoning over the unobserved intentions using model-based inference techniques our assistive system provides customized corrections on a user's issued commands. We present results from (1) a simulation-based study in which we validate our algorithm and (2) a 10-person human subject study in which we evaluate the performance of the proposed assistance paradigms. Our results suggest that (a) the corrective assistance paradigm helped to significantly reduce objective task effort as measured by task completion time and number of mode switches and (b) the assistance paradigms helped to reduce cognitive workload and user frustration and improve overall satisfaction.

Keywords Shared Autonomy, Assistive Robots, Interface-Aware Assistance

1 Introduction

In the assistive domain, human teleoperation of physically assistive robots (such as an assistive robotic arm or a powered wheelchair) is facilitated by control interfaces, such as a joystick, sip-and-puff or a switch-based head array that rely on unique physical mechanisms for their activation. The choice of interface is typically determined by the level of motor impairment and the residual motor function. For example, a person with low cervical-level spinal cord injury with residual hand function can use a joystick whereas a person with high-level spinal cord injury might be restricted to a sip-and-puff interface for which the physical interaction with the interface consists of exhaling and inhaling air through a sip-and-puff tube.

Typically, modeling of human teleoperation assumes that the human is always physically capable of issuing the intended control commands. However, this assumption is not always true in the assistive domain in the context of teleoperation of physically assistive robots because of multiple reasons: (1) inherent physical limitations of the user as a result of spinal cord injury or degenerative motor disease, (2) complexity of the device and (3) the physical modality of operating the interface.

*Equal contribution. Preprint under review.

Due to these limitations, quite often, the issued commands differ from the user’s intended commands. This can lead to sub-optimal or unintended robot behavior which in turn can increase user frustration and affect overall task performance detrimentally. In order to improve user acceptance of these assistive technologies and ensure high levels of performance and satisfaction, reasoning about and correcting for unintentional input commands become critical.

The control of a high-dimensional robot using low-dimensional control interfaces such as a switch-based head array or a sip-and-puff (Figure 1) necessitates the entire control space to be partitioned into smaller subsets called *control modes*. Due to this dimensionality mismatch between the machine and the control interface, the user must switch between these modes during manual teleoperation to fully control the system—this is referred to as *mode switching*. Mode switching adds an extra layer of *cognitive burden* because the user has to reason not only about the mapping from their input command to the desired robot action but also how the commands are partitioned through the interface. The cognitive load is further exacerbated due to the one-to-many mapping of the interface control command to the robot control command. In addition to the cognitive burden, there is also the *physical burden* of executing the mode switches until the desired mode is reached.



Figure 1: Sip-and-puff interface.

Unintentional mode switches, furthermore, are an issue when operating higher dimensional assistive machine using lower dimensional control interfaces. Unintentional mode switching arises from lack of perfect skill to control the interface, hardware issues that can arise due to regular wear and tear (for example, a faulty switch in a head array) and changing environmental circumstances (saliva accumulation in a sip-and-puff tube), fatigue and stress, among others. These accidental deviations can further exacerbate the burdens imposed on the user; it can add to the perceived task complexity and user frustration.

In this work, we address the question of how to accurately interpret the control command issued through a lower dimensional interface intended to control a much higher dimensional robot system. We introduce a personalized approach that models aspects of the interface and the human’s physical interaction with it and then uses these models to provide customized corrections on their issued commands.

Specifically, our contributions are threefold:

1. **Modelling Stochastic Deviations in User Input:** We mathematically formulate the user’s physical interaction with the control interface when teleoperating the robot—specifically how intended user inputs are filtered through the interface before being measured by the system. Furthermore, we use data collected from the user to build *user-specific* models of control mapping and stochastic deviations from intended commands to *personalize* the corrective algorithms.
2. **Model-Based Inference of Intended Input:** We develop a mathematical framework to perform model-based inference over unobservable intended user control commands. Assuming that we have some knowledge of the high-level control policy of the user, we use probabilistic reasoning over interface-level physical actions to reduce unintended deviations from optimal behavior.
3. **Customized Corrective Assistance:** We formulate two methods to provide appropriate corrections to the observed control signal in an *online* fashion. The results from our human subject study show that the assistance paradigms helped to improve objective task performance (as measured by task completion times and total number of mode switches) as well as reduce cognitive workload.

Since the personalized probabilistic models encode the idiosyncrasies of a particular user’s interaction behavior with the robot the assistance algorithms also are personalized to the user.

In Section 2 we present an overview of related research in the areas of intent inference, mode switch assistance and physical human teleoperation. Section 3 presents our mathematical formalism developed for reasoning about human’s intended interface-level physical actions. Section 4 describes the simulation-based experiments for validating the proposed assistance frameworks. Experimental design and study protocol are presented in Section 5 followed by results in Section 6. Discussion and conclusion are presented in Sections 7 and 8.

2 Related Work

Shared control assistive systems often require a good estimate of the user’s intent—which could be a high-level goal such as a navigation landmark a user might want to drive a wheelchair towards or an object on a table that a user intends to grab using an assistive robotic arm [1]. Bayesian inference based approaches are widely used in the context of shared-control in which the user is modelled as a Markov Decision Process and is assumed to be noisily optimizing

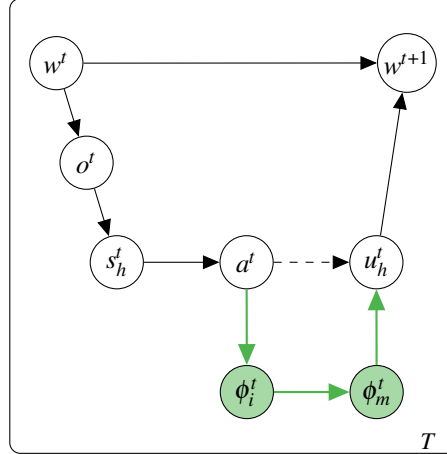


Figure 2: Probabilistic graphical model depicting a specific user’s interactions with the robot via the control interface at single time step t . The dashed edge between a^t and u_h^t indicates how typically teleoperation is modeled, which assumes that the user is physically capable of issuing the intended control command. The nodes and edges that model the physical aspect of controlling the interface is highlighted in green.

some cost function with respect to a high-level goal [2, 3]. In our work, we take a more fine-grained approach to modeling teleoperation in which we explicitly model the intended and measure interface-level physical actions and utilize Bayesian schemes to infer the intended interface-level actions from the measured user input.

Deviations between a person’s intended and executed actions can arise due to cognitive as well as physical factors [4]. For motor-impaired people, the inherent physical limitations can increase the likelihood of accidental deviations from intended commands which can lead to unwanted robot behavior. Therefore, in a shared-control human-machine system it is important for the autonomy to make decisions based on *intended* as opposed to executed actions to improve the quality of interaction; thus the need for action-level intent inference. Work in driver behavior modeling has investigated action-level inference, for example, to classify and predict driver actions [5]. Similarly, by combining ideas from semantic scene understanding and optimal control theory researchers have addressed the problem of *activity forecasting* to infer future actions of pedestrians from noisy visual input [6]. Some previous work has looked at modeling a person’s internal beliefs about a dynamic system, and uses an internal-to-true dynamics transfer function in order to provide the assistance that leads to a desired human action or desired human or learning [7, 8]. In these works it is assumed that any “suboptimal” human command is due to a mismatch between their internalized and the true dynamics model. There is no control sharing, the autonomy is always issuing commands based on what it infers the user wants to do. Another work considers the uncertainty in intent inference and reasons about intent ambiguity to provide appropriate autonomous planning and assistance [9].

3 Mathematical Formalism

In this section we describe our mathematical model of the user’s physical interaction with a control interface during manual teleoperation. Additionally, we present our assistive algorithm which uses our model to provide customized corrections on the user’s issued commands.

3.1 Modeling The User’s Physical Interface Operation

We use a dynamic Bayesian network to model the user’s physical interaction with a control interface during teleoperation of the robot. Figure 2 depicts the probabilistic graphical model for a user at a single time step t .

Let w^t represents the true world state and o^t the partial observation of the world state. The world state is partially observable due to various reasons; for example line of sight occlusions, lack of transparency, limited sensors, among others.² s_h^t denotes the internal state of the human as informed by the observation o^t and furthermore encodes the user’s internal goals and beliefs about the world. a^t represents the action primitives that are typically defined in the task space that the user intends to execute at time step t . u_h^t is the low-level human control command issued to the robot.

²In this paper, we assume that the world state is fully observable, such that $w^t = o^t$, but distinguish between w^t and o^t for completeness.

ϕ_i^t is the *intended interface-level physical action* initiated by the user that aims to achieve a^t and is *unobservable*. The exact nature of the physical action is interface dependent as different interfaces use different physical modalities for activation. ϕ_m^t is the *measured interface-level physical action* produced by the user that is fully *observable*. The novel contribution of our work is in distinguishing the unobservable ϕ_i^t from the measured ϕ_m^t and in explicitly modeling the physical mechanisms that generates u_h^t . Ideally, in a noise-free setting, ϕ_i^t and ϕ_m^t are equivalent. However, in reality ϕ_m^t may deviate from ϕ_i^t due to biases resulting from motor-impairment, stress, or fatigue. The importance of this distinction is that although the user expects ϕ_i^t to cause the world state w^t to transition to w^{t+1} in actuality ϕ_m^t causes the transition. This discrepancy can lead to transitions into undesirable world states which can induce user frustration.

We model the interactions between these variables within a probabilistic graphical model. Specifically, $p(\phi_i^t|a^t)$ captures the user’s *internal model* of the true mapping (which is static and deterministic and denoted as f) from task-level action primitives to the intended interface-level physical actions. Users acquire this internal model via training. $p(\phi_m^t|\phi_i^t)$ captures the stochastic deviations in the user’s physical actions when using the control interface. This conditional probability distribution can be interpreted as a user input *distortion* model. These conditional probabilities can be personalized by fitting the distributions to user-specific teleoperation data.

In this work we focus on the uniquely difficult problem of using a 1-DoF sip-and-puff interface to control a high dimensional³ robot. With a sip-and-puff, the likelihood of issuing unintended mode switches is quite high because of (1) cyclical mode switching (2) same method of input for motion control and mode switching (3) inherent difficulty in breath regulation and (4) factors such as fatigue, stress, and saliva gathered in the straw. For the sip-and-puff interface the set \mathcal{A} of action primitives consists of four discrete options. These options are: (1) clockwise mode switch (2) counter-clockwise mode switch 3) positive direction motion and 4) negative direction motion. Our implementation uses the sip-and-puff to operate three control modes: motion along x , y or θ . Depending on the active control mode the positive direction could be mapped to *right*, *up* or *clockwise* commands and the negative direction to *left*, *down* or *counter-clockwise* commands. Similarly, the set Φ of interface-level physical actions available for a sip-and-puff interface has four distinct options: 1) hard sip 2) soft sip 3) hard puff and 4) soft puff. The true mapping from action primitives to interface-level physical actions is deterministic (denoted as $f(\cdot)$) and predefined (as depicted in Figure 3), and users learn this mapping through practice.

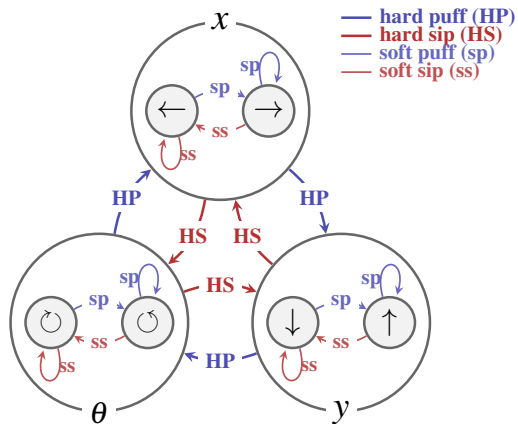


Figure 3: Sip-and-puff state-machine showing the set of high level actions (left, right, up, down, clockwise and counter clockwise rotation, and mode switching), low level control commands (hard puff, hard sip, soft puff, soft sip), and modes (x , y , and θ).

3.2 Estimation of a^t from measured ϕ_m^t

We are interested in the following question: given the measured interface-level physical action issued by the user ϕ_m^t what is the probability distribution over the task-level action primitives a^t ? More precisely, we are interested in the probability distribution $p(a^t|\phi_m^t)$. Concretely, using Bayes theorem, we have

$$p(a^t|\phi_m^t) \propto p(\phi_m^t|a^t)p(a^t) \quad (1)$$

³We define a high dimensional robot as one with more than two degrees of freedom.

Marginalizing over ϕ_i^t we have,

$$p(\phi_m^t | a^t) = \sum_{\phi_i^t \in \Phi} p(\phi_m^t, \phi_i^t | a^t) \quad (2)$$

Due to the conditional independence of a^t and ϕ_m^t Equation 2 becomes

$$p(\phi_m^t | a^t) = \sum_{\phi_i^t \in \Phi} p(\phi_m^t | \phi_i^t) p(\phi_i^t | a^t) \quad (3)$$

and plugging Equation 3 in Equation 1 we have,

$$p(a^t | \phi_m^t) = \eta p(a^t) \sum_{\phi_i^t \in \Phi} p(\phi_m^t | \phi_i^t) p(\phi_i^t | a^t) \quad (4)$$

where η is the normalization factor. We also have

$$p(a^t) = \sum_{s_h^t \in \mathcal{S}_h} p(a^t | s_h^t) p(s_h^t) \quad (5)$$

and combining Equation 5 with Equation 4 we have

$$p(a^t | \phi_m^t) = \eta \sum_{s_h^t \in \mathcal{S}_h} p(a^t | s_h^t) p(s_h^t) \left[\sum_{\phi_i^t \in \Phi} p(\phi_m^t | \phi_i^t) p(\phi_i^t | a^t) \right]. \quad (6)$$

3.3 Interpreting conditional probability distributions

Each one of the three conditional probability distributions that appear in the right hand side of Equation 6 have intuitive interpretations.

$p(a^t | s_h^t)$ is the *control policy* the user maintains internally. A novice user’s control policy could be a random policy initially, due to lack of familiarity with or understanding of how the system works. With training, practice, and learning, the user’s policy will gradually converge to an optimum—with respect to an internal cost function [10, 11, 12].

$p(\phi_i^t | a^t)$ captures the user’s *internal model* of the mapping from task-level action primitives to the intended interface-level physical actions. Users acquire an internal model of this mapping (which is static and deterministic) via training [13]. For example, when using a 2-DoF linearly proportional joystick to control a 2-D wheelchair, the control-mapping from the action primitive to interface-level physical actions is intuitive to most people (to move the wheelchair forward, deflect the joystick forward; to move forward faster, deflect the joystick forward more). However, using a sip-and-puff interface can be less intuitive because the physical actions (regulating air pressure while blowing into and sucking from a tube) do not have a one-to-one correspondence to the task-level action primitives and are less transparent to the user.

Lastly, $p(\phi_m^t | \phi_i^t)$ captures the stochastic deviations of the *measured* interface-level physical actions from the *intended* interface-level physical actions. This conditional probability distribution can be interpreted as the user input *distortion* model. These deviations can be due to fatigue, delayed or faulty memory retrieval, or features of the interface.

These conditional probabilities can be personalized by fitting the distributions to user-specific teleoperation data.

3.4 Customized Handling of Unintended Physical Actions

The motivation for our framework described in Section 3.2 is to improve the control of complex robotic machines with limited interfaces used by people with motor-impairments. The derived probabilistic measure of the true human action intent can be used within a shared-control assistive paradigm to provide corrective measures to reduce the cognitive and physical burden of unintentional mode switches. The inference scheme is outlined in Algorithm 1. Using Equation 6, at every time step t we compute the likelihood of $a^t \in \mathcal{A}$ conditioned on the observed ϕ_m^t (line 2). The action primitive corresponding to the maximum of the distribution is chosen as the intended action $a_{intended}^t$, and using the true control mapping function f we compute $\phi_{intended}^t$ (lines 3-4). In Algorithm 2, the system chooses to intervene only if $\phi_{intended}^t$ is different from ϕ_m^t and the uncertainty of prediction, computed as the entropy H of the distribution, is less than a pre-defined threshold ϵ . Otherwise, the measured interface-level physical action will be passed through the pipeline unimpeded. The appealing characteristic of our proposed control-sharing algorithm is that the user is maximally in control. When the autonomy does step in, it does so only to provide commands closest to the user’s true intentions (which they were unable to issue correctly themselves). Having the user maximally in control can potentially improve user satisfaction and acceptance [14].

We implement and evaluate two corrective assistance shared-control paradigms.

Algorithm 1 Infer Intended Commands

```
1: procedure INFER_INTENDED_COMMAND( $t, \phi_m^t$ )
2:   compute  $p(a^t | \phi_m^t)$  ▷ equation 6
3:    $a_{intended}^t \leftarrow \operatorname{argmax}((p(a^t | \phi_m^t)))$ 
4:    $\phi_{intended}^t \leftarrow f(a_{intended}^t)$  ▷ true control mapping
5:   return  $\phi_{intended}^t$ 
6: end procedure
```

Algorithm 2 Handle Unintended Commands

```
1: procedure HANDLE_UNINTENDED_COMMANDS( $t, \phi_m^t$ )
2:    $\phi_{intended}^t = \text{INFER\_INTENDED\_COMMAND}(t, \phi_m^t)$ 
3:   if  $\phi_{intended}^t \neq \phi_m^t$  then
4:     if  $H(p(a^t | \phi_m^t)) < \epsilon$  then ▷ uncertainty is low
5:       if filter_based_assistance then
6:          $\phi_{corrected}^t = 0$ 
7:       else if corrective_based_assistance then
8:          $\phi_{corrected}^t = \phi_{intended}^t$ 
9:       end if
10:    else
11:      return  $\phi_m^t$ 
12:    end if
13:  else
14:    return  $\phi_m^t$ 
15:  end if
16:  return  $\phi_{corrected}^t$ 
17: end procedure
```

3.4.1 Filtering autonomy

Conditioned on the uncertainty in the prediction, if ϕ_m^t is deemed as unintended, filter (or block) this command. In our implementation this means that $\phi_{corrected}^t = 0$ (i.e. no motion or mode-switching occurs as a result of this command).

3.4.2 Corrective autonomy

Conditioned on the uncertainty in the prediction, if ϕ_m^t is deemed as unintended, $\phi_{corrected}^t = \phi_{intended}^t$ (i.e. the control command that will result in the intended action).

4 Simulation-based Algorithm Evaluation

In order to gain a deeper insight into how different hyper-parameters—such as noise levels in $p(\phi_i^t | a^t)$ and $p(\phi_m^t | \phi_i^t)$ —affect the overall performance of our proposed assistance algorithm, we designed a simulation-based experiment in which the model shown in Figure 2 was used as a generative model from which task-level action primitives (a^t) and intended interface-level physical actions (ϕ_i^t) were sampled. ϕ_i^t was corrupted according to the user distortion model $p(\phi_m^t | \phi_i^t)$ to generate ϕ_m^t . In our simulations, we assumed full observability of the world state (that is, $o^t = w^t$) and the existence and knowledge of a fully deterministic optimal policy (i.e. $p(a^t | s_h^t)$ is known).

The human teleoperation of the robot using the control interface was modeled as a Markov Decision Process where the world state $w^t \in \mathcal{W}$ was defined as a 3-tuple (p_n^t, θ^t, m^t) , where $p_n \in [p_0 \dots p_{N+1}]$ denoted discrete locations that represented the way-points (including the start and end) of the path (similar to the path shown in Figure 5), N was the number of turns, $\theta^t \in [0, -\pi/2, \pi/2]$ was the discrete orientations available to the point robot and $m^t \in [m_1, m_2, m_3]$ denoted the currently active mode. The action space \mathcal{A} was identical to the space defined at the end of Section 3.1. For a perfect agent, $p(\phi_i^t | a^t)$ and $p(\phi_m^t | \phi_i^t)$ are delta distributions (due to lack of any distortion or noise). In reality due to various factors such as stress, fatigue or hardware issues, these distributions can become noisy. In the simulations, the amount of random noise injected into $p(\phi_i^t | a^t)$ and $p(\phi_m^t | \phi_i^t)$ was treated as a simulation parameter. Table 1 indicates the ranges of all parameters used in the simulation experiments.

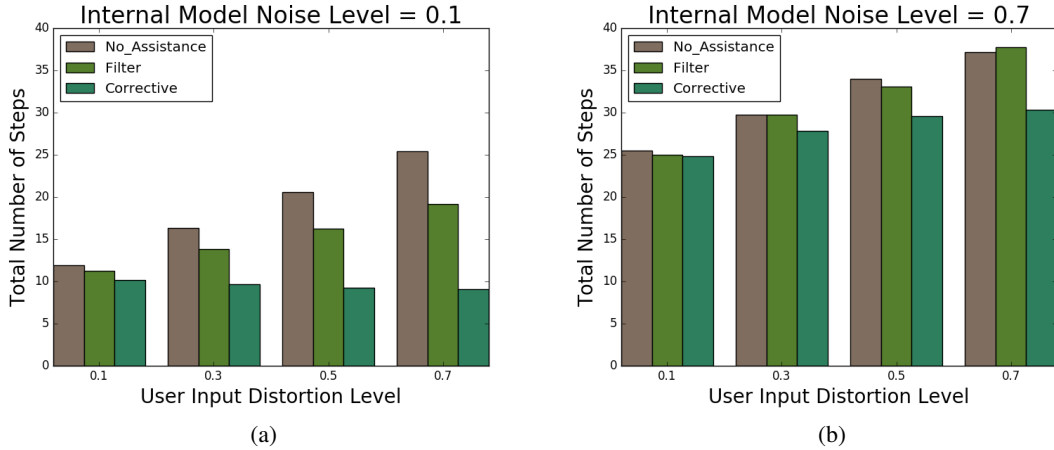


Figure 4: Total number of state transitions for two different noise levels in $p(\phi_i|a)$ - 0.1 (left) 0.7 (right).

Parameter	Range of Values
N	[1,2,3]
Assistance Type	[Filter, Corrective, No Assistance]
Noise in $p(\phi_i a)$	[0.1, 0.3, 0.5, 0.7]
Noise in $p(\phi_m \phi_i)$	[0.1, 0.3, 0.5, 0.7]

Table 1: Ranges of different simulation parameters.

Table 2: Prediction Accuracy of Intended Commands (%)

$p(\phi_i a)$ noise	$p(\phi_m \phi_i)$ noise			
	0.1	0.3	0.5	0.7
0.1	84.5	87.8	90.6	91.5
0.3	62.6	60.6	61.1	58.8
0.5	52.5	47.8	46.9	46.0
0.7	45.3	41.6	39.9	39.4

We evaluated the performance of our assistance algorithm as measured by the total number of state transitions during a trial under different assistance conditions and investigated the effect of different levels of random noise in $p(\phi_i^t|a^t)$ and $p(\phi_m^t|\phi_i^t)$ on the amount of assistive intervention and accuracy of intent prediction (Figure 4).

Figure 4 reveals that a more accurate internal model (i.e. the mapping from task-level action primitives to interface-level physical actions), in general, will help the user perform better. For a given internal model, the corrective assistance paradigm has the highest performance followed by filtering and no-assistance. The difference in performance between the assistance paradigms decreases as the internal model becomes noisy, illustrating the need for proper training and acquisition of accurate internal models. These insights helped us design the proper experimental protocol which will be explained in detail in the next section. Table 2 and Table 3 indicate that the prediction accuracy and percentage of assistive interventions is more sensitive to noise in $p(\phi_i|a)$ than $p(\phi_m|\phi_i)$, once again reinforcing the need for proper training for the user so that they acquire a good understanding of the true mapping from action primitives to interface-level physical actions.

5 Experimental Design

To evaluate our inference algorithm and assistive paradigms, we ran a human-subject study ($n = 10$). All participants gave their informed, signed consent to participate in the experiment, which was approved by Northwestern University’s Institutional Review Board. Each study session consisted of three phases:

1. Phase 1: Training and data collection to model personalized $p(\phi_i^t|a^t)$.

Table 3: Percentage of Assistive Interventions (%)

$p(\phi_i a)$ noise	$p(\phi_m \phi_i)$ noise			
	0.1	0.3	0.5	0.7
0.1	16.2	28.8	35.2	39.6
0.3	10.9	18.3	24.1	27.3
0.5	10.6	13.2	17.3	21.0
0.7	10.9	12.0	14.8	17.3

2. Phase 2: Training and data collection to model personalized $p(\phi_m^t|\phi_i^t)$.
3. Phase 3: Assistance evaluation phase in which the subjects controlled a 3D point robot using the sip-and-puff interface under three distinct assistance conditions.

5.1 Personalized Distributions

We designed two tasks to capture the personalized distributions $p(\phi_i^t|a^t)$ and $p(\phi_m^t|\phi_i^t)$ from user studies.

5.1.1 Personalized Internal Control-Mapping Model

Participants were first trained on the “true” mapping during a standardized training phase. The training phase consisted of three phases: (1) learning about the action primitives for the 3-D experimental task-space (Figure 5), (2) learning about the interface-level physical actions available through the interface, and (3) how these commands are partitioned through the selected interface (Figure 3). The training was followed by the testing phase. During testing, the user was shown a graphical depiction of an action primitive, and instructed to select the correct interface-level physical action that would result in a^t . The testing consisted of six blocks. Each block consisted of all the available actions in a randomly balanced order. To account for the effect of time-induced stress on $p(\phi_i^t|a^t)$, each of the three blocks had a time limit of five seconds. Stress can affect memory retrieval, and time constraints have been shown to be the main limitation of working memory since processing and storage compete for limited resources [15]. A training refresher was given between blocks. The distribution $p(\phi_i^t|a^t)$ was modeled using data collected during the testing phase in which we assumed that the user’s internal model is quasi-stationary. The subjects had to repeat the training and the testing protocol until they met a minimum level of proficiency. This was to ensure that when subject performed the simulation study in Phase 3, they had a good understanding of what physical actions were needed to generate the required low-level commands to successfully complete the trial.

5.1.2 Personalized User Input Distortion Model

We designed a second task to model the stochasticity in the user’s interface-level physical action. The user was coached on the operation of the interface during a training phase in order to ensure good understanding of physical aspects of using the interface. During testing, the user was shown a command on the screen (e.g. “Soft Puff”) and asked to issue the same command through the interface. Similar to the experiment in Section 5.1.1, to monitor the effect of time-induced stress on $p(\phi_i^t|\phi_m^t)$, each trial had a time limit of five seconds. The distribution $p(\phi_m^t|\phi_i^t)$ was modeled using the data collected during this testing phase.

5.2 Assistance Evaluation

We designed a simulation-based task (Figure 5) for evaluating the assistive shared-control paradigms.⁴ In this task, the subject controlled the motion of a 3-DoF point robot along pre-defined path from a start pose to a goal pose. The optimal number of mode switches to complete the task was known. For each trial, the start and end positions were randomized. The initial mode was random, but different from the optimal mode the user had to be in for performing the first movement. Users performed the evaluation task under three conditions: (1) *no assistance*, (2) *filtering* assistance, and (3) *corrective* assistance. The subject was required to rotate the point robot to the target orientation at one of the corners (highlighted in violet). Subjects were prompted to complete the task efficiently (i.e. least number of mode switches and in a timely manner). Each trial had a maximum time limit of 50 seconds. Feedback regarding the current active mode was displayed on the screen (on the top right corner). Subjects performed six blocks (two blocks per assistance condition) of trials. Each block consisted of six trials for a single assistance condition. In total, we collected

⁴Code available at https://github.com/argallab/corrective_mode_switch_assistance.git

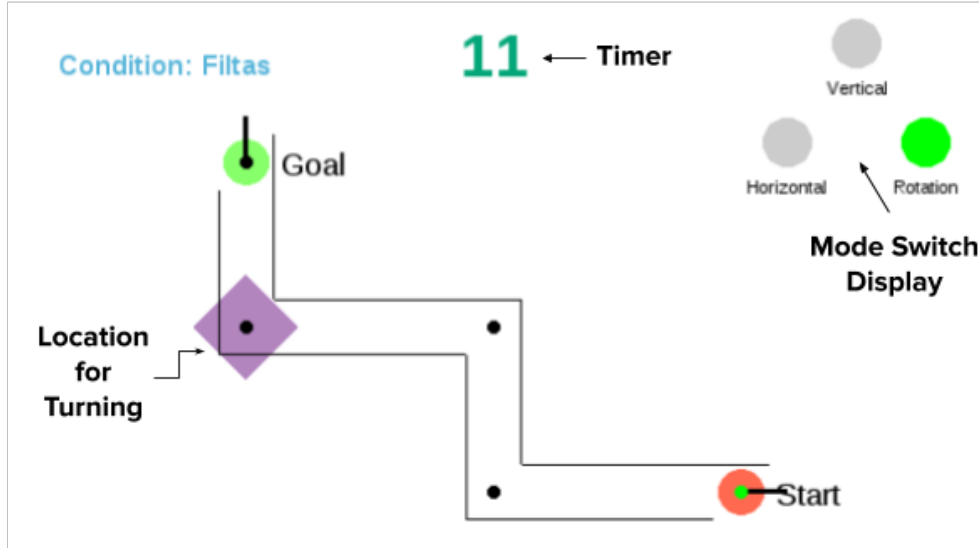


Figure 5: Pictorial representation of the simulated environment used in our human-subject study.

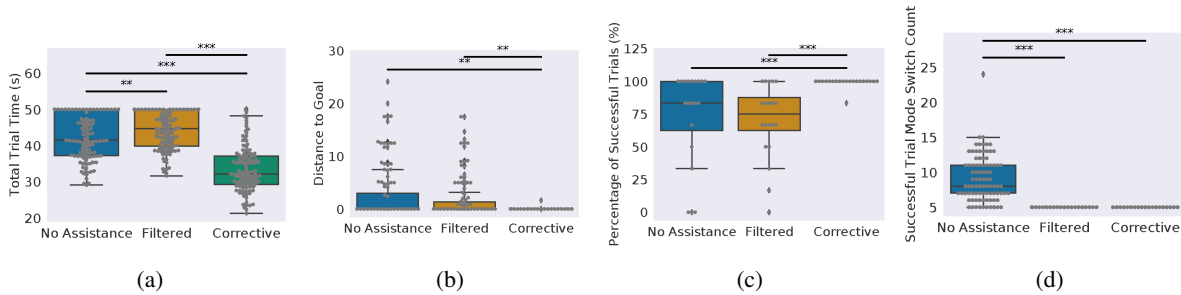


Figure 6: Objective task performance metrics grouped by assistance condition. (a) Total trial time with maximum trial time capped at 50s, (b) distance to the goal at the end of trials, (c), percentage of successful trials, (d) total number of mode switches during successful trials. The optimal number of mode switches was 5 for all trials. All metrics improve significantly (***) : $p < 0.001$) with the corrective assistance condition.

360 trials (120 trials per assistance condition). After each block, the subjects were required to respond to a NASA-TLX questionnaire. At the end of the sixth block, the subjects also filled out a post-session survey in which they rank ordered the different assistance conditions according to their preference, intuitiveness, helpfulness, and difficulty.

6 Results

First we present the statistical analysis of the objective metrics of task performance compared across the three assistive conditions, followed by the subjective measures and user preferences. We analyze group performances using the non-parametric Kruskal-Wallis test and perform the Conover’s test post-hoc pairwise comparisons to find the strength of significance. For all figures, the notation * implies a p-value of $p < 0.05$, ** implies $p < 0.01$, and *** implies $p < 0.001$.

6.1 Objective Task Performance Metrics

To evaluate the effectiveness of our algorithm on overall task performance, we compared (1) the total task completion times, (2) the distance to the desired goal position and orientation at the end of each trial, (3) the percentage of successful trials under each assistance condition, and (4) the total number of mode switches for successful trials, compared across the three assistance conditions (Figure 6).

As seen in Figure 6a, the total trial time is largest under *filtered* assistance, reduces with *no assistance* and is the lowest under the *corrective* assistance paradigm. In the *filtered* assistance condition, the algorithm forces the user to switch mode in an optimal manner at all times. Repeated issuance of sub-optimal commands (mode-switching in the wrong direction) will always be blocked due to strict enforcement of optimal number of mode switches and would

result in increased task completion time. It is also likely that, under the *filtered* assistance paradigm, the subject could get confused about why an issued command was filtered out and could resort to ‘forcing’ behavior (similar to how people repeatedly press elevator buttons while waiting in order to ‘force’ the elevator to come sooner). However under the *no assistance* condition, the subject could end up in the desired control mode by executing multiple consecutive sub-optimal mode switches in quick succession. Specifically, in our experimental setup, two counter-clockwise mode switches is equivalent to a single clockwise mode switch and vice versa. As a result, the number of mode switches will typically increase (as seen in Figure 6d), however the task completion time could remain relatively small.

Figures 6b-6c show the distance to goal at the end of the trial and the percentage of trials successfully finished by each subject, respectively. Both of these metrics improve significantly under the *corrective* assistance condition, however, there is no statistically significant difference between the *filtered* assistance and *no assistance*. With *corrective* assistance, almost all users have a 100% success rate, therefore it is expected that the distance to goal will be zero.

The *filtered* and *corrective* assistance paradigms are comparable when looking at the total number of mode switches during only successful trials, as shown in Figure 6d. The optimal number of mode switches for all trials is five, and we see both assistive paradigms are optimal with respect to the number of mode switches. However, under *no assistance*, even if the trial was successfully completed, the number of executed mode switches was up to three times the optimal number required.

6.2 Subjective Task Performance Metric

We use the raw NASA-TLX as a subjective measure of perceived workload since it is an established and reliable metric [16]. A larger TLX score indicates a higher perceived workload. Although during filtered assistance, the autonomy gives feedback to the user by way of blocking unintended actions, the user is still fully responsible for all issued commands. During corrective assistance, the autonomy offloads some of the cognitive burden by correcting unintended actions, and as a result also offloading the physical burden of corrections, without the user’s awareness. This significantly reduces the user’s perceived workload, as seen in Figure 7.

6.3 User Acceptance of Assistive Autonomy

Finally, we evaluated user preferences and acceptance of our shared-control assistive paradigm using a post-task questionnaire, summarized in Figure 8. The statements were rated on a 7-point Likert scale from strongly disagree (1) to strongly agree (7). Although the objective measures of task performance between *filtered* assistance and *no assistance* were comparable, the users felt that the *filtered* assistance helped them complete the task more efficiently and was easier to operate than under *no assistance*. Overall, the participants strongly agreed that the *corrective* assistance helped reduce unwanted mode switches and did not make them fatigued.

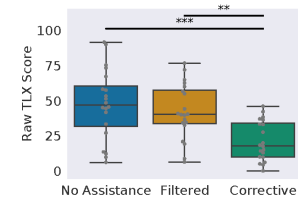


Figure 7: Perceived workload measured by the NASA-TLX score, grouped by assistance condition.

7 Discussion

7.1 Implications for Shared Control

The assistance paradigms presented in this work can potentially help users improve their interface operation skills and achieve high-levels of task performance. Since the *filtering* assistance blocks all user input that do not correspond to optimal actions, a user operating the interface under this condition will learn to issue the correct commands, thereby improving overall teleoperation skill. On the other hand, the *corrective* assistance paradigm is more effective in situations where efficient and successful task completion is more critical (for example, crossing a street on a powered wheelchair). Each of the assistance paradigms has its own advantages and when used in tandem can drastically improve the overall quality of human teleoperation of a physically assistive device.

7.2 Future Work

One of the assumptions in our current framework is that the subject’s internal mapping $p(\phi_i|a)$ is stationary. We currently ignore how learning can improve the internal model thereby changing the baseline performance. On the other hand, fatigue and hardware related issues can potentially make $p(\phi_m|\phi_i)$ more noisy during the course of a session. In our future work, we intend to explicitly model fatigue and learning dynamics and their impact on each of

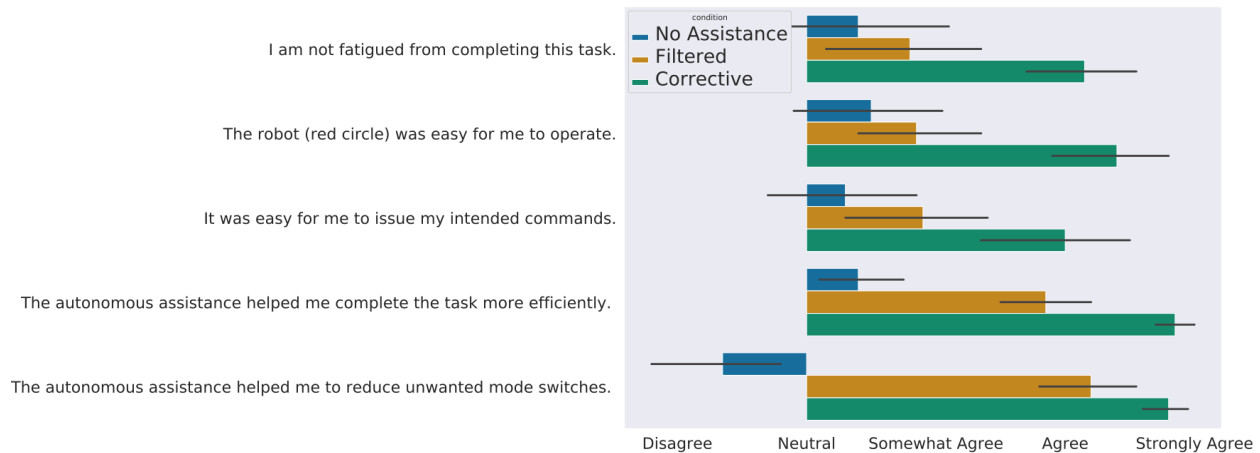


Figure 8: Average user response to post-task questionnaire. The bars indicate standard deviation.

the personalized distributions. Another observation that is not reflected in our analysis is how subjects altered their control strategies depending on the assistance conditions. In the *corrective* assistance condition, some subjects realized that even a ‘wrong’ command resulted in intended task-level action and then proceeded to exploit this feature. Our future work will address the best way to adapt the assistance provided based on whether the user is truly attempting to provide the appropriate input or not.

8 Conclusion

In this paper we describe a mathematical framework based on dynamic Bayesian Networks to model the user’s physical interaction with the control interface during robot teleoperation. We also introduce two assistance paradigms that reason about the user’s intended commands and provide corrective behaviors. A simulation-based experiment was performed to validate the efficacy of our algorithm. The assistance paradigms were evaluated using a ten person human subject study. Our results indicate that the assistance conditions were helpful in improving various objective task metrics such as task completion times, number of mode switches performed, distance to goal and percentage of successful trials. More importantly, the assistance paradigms also reduced the perceived cognitive workload and user frustration and improved user satisfaction.

References

- [1] Dylan P. Losey, Craig G. McDonald, Edoardo Battaglia, and K O’Malley, Marcia. A review of intent detection, arbitration, and communication aspects of shared control for physical humanrobot interaction. *Applied Mechanics Review*, 2018.
- [2] Henny Admoni and Siddhartha Srinivasa. Predicting user intent through eye gaze for shared autonomy. In *2016 AAAI Fall Symposium Series*, 2016.
- [3] Shervin Javdani, Siddhartha S Srinivasa, and J Andrew Bagnell. Shared autonomy via hindsight optimization. *Robotics Science and Systems: Online Proceedings*, 2015, 2015.
- [4] Icek Ajzen, Thomas C. Brown, and Franklin Carvajal. Explaining the discrepancy between intentions and actions: The case of hypothetical bias in contingent valuation. *Personality And Social Psychology Bulletin*, pages 1108–1121, 2004.
- [5] Alex Pentland and Andrew Liu. Modeling and prediction of human behavior. *Neural Computation*, pages 229–242, 1999.
- [6] Kris M Kitani, Brian D Ziebart, James Andrew Bagnell, and Martial Hebert. Activity forecasting. In *European Conference on Computer Vision*, pages 201–214. Springer, 2012.

- [7] Siddharth Reddy, Anca Dragan, and Sergey Levine. Where do you think you're going?: Inferring beliefs about dynamics from behavior. *Neural Information Processing Systems (NeurIPS)*, 2018.
- [8] Anna N. Rafferty, Michelle M. LaMar, and Thomas L. Griffiths. Inferring learners knowledge from their actions. *Cognitive Science*, page 584618, 2015.
- [9] Michael Bowman, Songpo Li, and Xiaoli Zhang. Intent-uncertainty-aware grasp planning for robust robot assistance in telemanipulation. *International Conference on Robotics and Automation (ICRA)*, pages 409–415, 2019.
- [10] Masao Ito. Internal model visualized. *Nature*, pages 153–154, 2000.
- [11] Richard J. Jagacinski and A. Miller, Richard. Describing the human operators internal model of a dynamic system. *Human Factors*, pages 425–433, 1978.
- [12] Joann Kluzik, Jörn Diedrichsen, Reza Shadmehr, and Amy J. Bastian. Reach adaptation: What determines whether we learn an internal model of the tool or adapt the model of our arm? *Journal of Neurophysiology*, pages 1455–1464, 2008.
- [13] Camilla Pierella, Maura Casadio, Sara A. Solla, and Ferinando A. Mussa-Ivaldi. The dynamics of motor learning through the formation of internal models. *PLOS Computational Biology*, 2019.
- [14] Alex Broad, Todd Murphey, and Brenna Argall. Highly parallelized data-driven mpc for minimal intervention shared control. *In Proceedings of Robotics: Science and Systems (RSS)*, 2019.
- [15] Pierre Barrouillet, Sophie Bernardin, and Valérie Camos. Time constraints and resource sharing in adults working memory spans. *Journal of Experimental Psychology: General*, pages 83–100, 2004.
- [16] S. G. Hart. NASA-task load index (NASA-TLX); 20 years late. *Proc. of the Human Factors and Ergonomics Society Annual Meeting*, pages 904–908, 2006.